Crystallographic Effects on Nano-plasticity on Copper Surfaces

H. Y. Liang[1], C. H. Woo[1], Hanchen Huang[2]

Summary

Molecular dynamics (MD) simulation is carried out to study the loading and unloading behavior of nano-indentation on copper surfaces as a function of crystallographic orientation. The differences in the deformation and recovery behavior of the three surfaces are investigated, and found to be attributable to the different underlying dislocation structures resulting from the crystallographic anisotropy. At small indentation depths, dislocation-induced plasticity can sometimes be completely recovered upon unloading. The origin and implication of this recovery are discussed.

Introduction

Crystalline plasticity has been an active research field with a long history. Besides being of obvious scientific interest, the understanding of plasticity on surfaces of crystalline materials in the nanoscale is also of technological importance, due to the rapid development of nanotechnology in recent years. In this regard, experiments are performed to study the complex surface deformation behavior under the applied stress of a nano-indenter. However, due to the many contributing factors that need to be considered, such as the size and tip geometry of the indenter, penetration depth, surface oxide layer and contamination, elastic anisotropy of substrate, time-dependent characteristics, and strain gradient effects etc., an unambiguous interpretation of the results is not often achievable [1-4]. To complement the experiments and to better understand the changes that occur to the material beneath the surface under the nano-indenter, from which the deformation is derived, atomistic simulations are conducted (see [5-9] for example).

While existent calculations mostly concentrate on the loading part of the indentation process, the understanding of nano-plasticity cannot be complete without the unloading part of the story. However, the dependence of the unloading behavior on the loading history makes a systemic study very time consuming. Nevertheless, in this paper, we report our initial attempt in this

[1] Department of Mechanical Engineering, Hong Kong Polytechnic University, Hong Kong SAR, China
[2] Department of Mechanical, Aerospace & Nuclear Engineering, Rensselaer Polytechnic Institute, Troy, NY 12180, USA

direction. Starting from a copper surface in one of the three crystallographic orientations, (001), (110), and (111), indented to various depths, the load-displacement curve of unloading is obtained, using MD simulation. Copper is chosen as our prototype material because of its strong elastic anisotropy, and its readily available and relatively reliable interatomic potential,

Simulation Procedure

Three copper substrates with (001), (110), and (111) surfaces are modeled as slabs. For Cu (001), the dimension is $188 \times 188 \times 108$ Å^3 (containing 324,480 atoms), the top free surface is (001) plane, and the other two horizontal directions are (100) and (010) respectively. For Cu (110), the dimension is $189 \times 187 \times 112$ Å^3 (containing 338,624 atoms), the top surface is (110) plane, with the other two side surfaces $(\bar{1}10)$ and (001) respectively. For Cu (111), the dimension is $190 \times 189 \times 112$ Å^3 (containing 341,334 atoms), the top surface is (111) plane, with the other two side surfaces are $(\bar{1}10)$ and $(\bar{1}\,\bar{1}2)$ respectively. The simulation procedure, using an indentation velocity of 3 m/s, is the same as that discussed in detail previously [5], and will not be repeated here.

Results and Discussions

The load-displacement curves, i.e., force (F) vs. indentation depth (h), for indentation on the three crystallographic surfaces (001), (110), and (111) are compared in Fig.1, for both the loading and unloading cases. F is the load applied to push the indenter. The indentation depth (h) is the prescribed displacement of the indenter, which is related to the movement of the spherical indenter center. By definition, h is zero on the undeformed surface. We note that the actual depth is smaller than the prescribed indenter displacement due to the compliance of a real indenter.

Fig.1a shows the strong effects of the crystallographic anisotropy on the reduced modulus along different crystallographic directions. Apart from the effects on the reduced modulus, the resulting elastic anisotropy also influences the stress distribution under the indenter as well. In [10], the stress distribution, calculated from three-dimensional FEM analyses of a stiff frictionless spherical indenter pressing onto substrates corresponding to Cu (001), (110), and (111), is compared with the atomic stress tensor [11] calculated from the MD simulation results. Despite the vast difference between the two models, the qualitative resemblance between FEM and MD results shows remarkable consistency. Thus, in the elastic regime, the discrete lattice can still be described satisfactorily as a continuum, despite the highly concentrated local stresses.

In all the load-displacement curves in Fig.1, inflexion points can be seen beyond the elastic regime, during loading or unloading. In Figs. 1b to 1d,

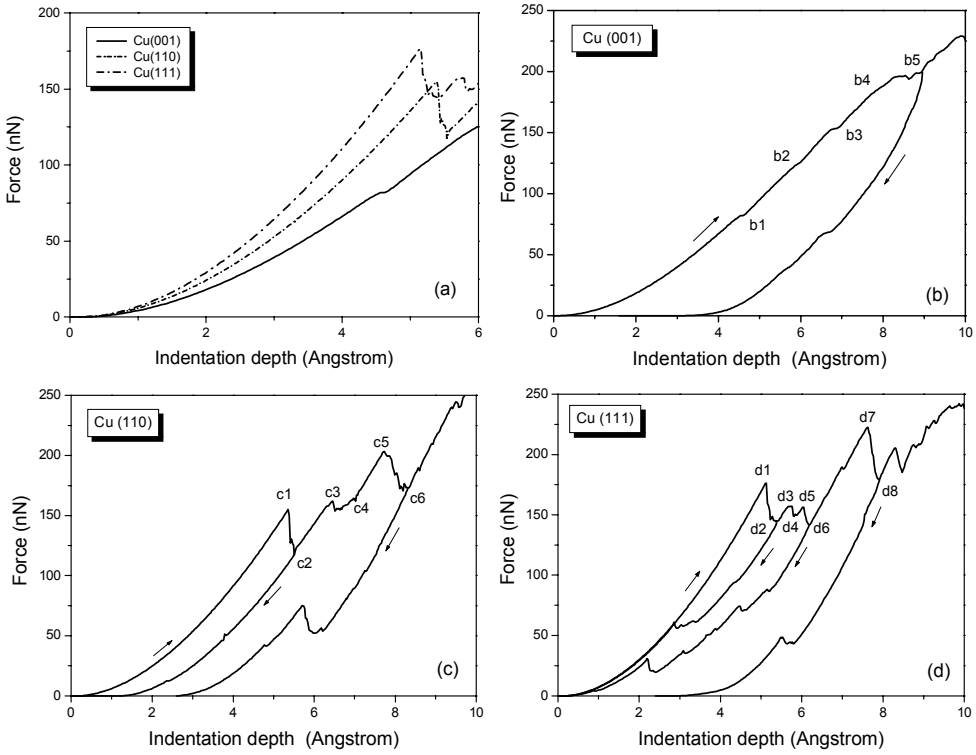

Figure 1: Load-displacement curve of Cu (001), (110), and (111), on loading and unloading.

arrows pointing in the direction of increasing depth (h) indicate loading, and those pointing in the direction of decreasing depth indicates unloading. Roughly speaking, unloading from different points on the loading curve shows that indentation to smaller depths is completely recoverable, and that to larger depths is not.

The load-displacement curve for Cu (001) is shown in Fig.1b. On loading, there are five inflexion points, #b1 to #b5, in the shape of yielding platforms, produced by minor yielding due to inelastic deformation under the indenter. Between the inflexion points, the curve shows a relatively stable and smooth quasi-elastic behavior, corresponding to a steady build up of internal stress, consistent with a relatively inactive dislocation structure. If the specimen is unloaded before the indenter reaches a depth of 0.69 nm, i.e., beyond point #b3,

the indentation can be fully recovered. Beyond a depth of ~ 0.89nm, i.e., point #b5, it becomes permanent. The deformation characteristics on loading have been discussed in detail in the case of Cu (100), and are well explained in terms of the dislocation structure evolution [5]. Referring to the dislocation structures at the various points #b1 to #b5 reported in [5], the present unloading behavior can also be understood. Thus, at a depth smaller than 0.69 nm, i.e., point#b3, the dislocation structure essentially consists of Lomer-Cottrell locks [5], which anneal out under the action of the surface image forces, as the applied force due to the indenter is gradually reduced. At deeper penetration to beyond 0.89 nm, i.e., point #b5, the evolution of the dislocation structure is similar to the usual cold-working process, in which dislocations are generated, interact, and lock together. Unloading at this stage does not get rid of all the dislocations. Residual deformation remains even when the applied stress due to the indenter is completely removed.

Most noticeable on the loading curve of Cu (110) in Fig.1c are the two large load drops, at points #c1 (h~5.4 Å and F~155.0nN) and #c5 (h~7.6 Å and F~203.2nN), due to a sudden relaxation of the internal stress supporting the indenter, such as that caused by the softening of the crystal initiated by the sudden nucleation of dislocations from a source. It is also noted that the relaxation here is associated only with a relatively small advancement of the indenter. Between the points #c3 and #c4 there is a yielding platform that involves a small stress relaxation, but a relatively large indenter advancement, probably caused by dislocation glide under a constant driving shear. The steadily rising parts of the curve between the points #c2 and #c3, #c4 and c5, and after point #6 again exhibit the typical quasi-elastic behavior, corresponding to the accumulation of internal stresses, caused by a relatively inactive dislocation structure. For Cu (110), the indentation cannot be recovered, even at the first load drop point #c2. The details of the evolution of the underlying dislocation structure will be published elsewhere, and will not be discussed here. It is sufficient to point out here that the atomistic picture shows the formation at #c2, of four interacting partials, in the form of two pairs of Lomer-Cottrell locks, which remains intact even when the indenter is removed, thus causing the residual plastic strain.

Similar to Cu (110), the load-displacement curve of Cu (111) in Fig.1d also shows two large load drops with little deformation at points #d1 (h~5.1 Å and F~176.3nN) and #d8 (h~7.7Å and F~222.3nN), caused by stress relaxation due to softening induced by intense dislocation activities. The region between points #d2 and #d6 exhibits a behavior similar to that between #c3 and #c4 in the Cu (110) case, namely a yielding platform that involves a small stress relaxation, but a relatively large indenter advancement, probably caused by dislocation glide under a constant driving shear. Between points #d6 and #d8, the curve rises again quasi-elastically, with a minor inflexion at points #d7,

corresponding to the accumulation of internal stress, caused by a relatively inactive dislocation structure. For Cu (111), despite the significant plastic deformation, all dislocations can be driven out of the substrate upon unloading, and the deformation can be fully recovered, before the indentation reaches a depth of beyond 0.6 nm, i.e., point #d6. Beyond a depth of 0.79 nm, i.e., point #d8, the dislocation structure contains many interacting segments, and the indentation cannot be completely recovered.

As a general observation, independent of the crystallography of the indented surface, three types of behavior can be seen from the load displacement curves: (1) quasi-elastic; (2) small displacement but large load drop (simply called load drop); and (3) large displacement under constant load (simply called strain burst). Experimentally, discrete load jumps or strain bursts with intermittent elastic response are typical features [12-13]. It is interesting to note in Fig.1 that while all three types of behaviors are present in the case of Cu (111) and (110), Cu (001) is dominated by the quasi-elastic behavior, interrupted only by several small strain bursts.

For all the unloading curves, inflexion and even "rebounding" points can be seen, indicating the annihilation of dislocations, which is attributable to the action of image forces due to the proximity of the sample surface. From a macro continuum viewpoint, except for plasticity due to phase transformations, most plasticity in bulk metals are dislocation induced and cannot be recovered. It is interesting that in the present cases, nevertheless, the dislocation-induced plasticity can be recovered.

The results here offer a potential explanation for the delayed type of pop-in observed previously in experiments [3]. It was found that if the load is held at a value too small to produce an instantaneous pop-in, a pop-in may occur after some waiting time. Although the present atomistic simulations were performed on a much smaller length scale compared to real nanoindentation experiments, the results here nevertheless show that at small loads, the loading and unloading may appear to be elastic, but at the same time defects can exist beneath the indenter and can unzip if the load is removed. These defects are therefore invisible to an experimentalist, unless the evolution of the as-loaded dislocation structure can be observed *in situ*. However, if the load is held, these defects, for example, the edge character Lomer-Cottrell lock, can climb, and when they reach a critical size they may act as spontaneous dislocation sources to result in a substantial strain burst.

Acknowledgement

The work described in this paper was supported by grants from the Research Grants Council of the Hong Kong Special Administrative Region (PolyU 1/99C, PolyU 5309/03E and PolyU 5312/03E).

References

[1]. Gouldstone, A., Koh, H.J., Zeng, K.Y., Giannakopoulos, and A.E., Suresh, S., (2000), *Acta Mater*., **48**, 2277.
[2]. Swadener, J.G., George, E.P., and Pharr, G.M., (2002), *J. Mech. Phys. Solids*, 50, 681.
[3]. Chiu, Y.L. and Ngan, A.H.W., (2002), *Acta Mater*., **50**, 1599-1611.
[4]. Gerberich, W.W., Tymiak, N.I., Grunlan, J.C., Horstemeyer, M.F., and Baskes, M.I., 2002, *J. Appl. Mech*., **69**, 433.
[5]. H. Y. Liang, C. H. Woo, Hanchen Huang, A. H. W. Ngan, T. X. Yu, (2003) *Philos. Mag.***83,** 3609.
[6]. Zimmerman, J.A., Kelchner, C.L., Klein, P.A., Hamilton, J.C., and Foiles, S.M., 2001, *Phys. Rev. Lett*., **87**, 165507.
[7]. Rodríguez de la Fuente, O., Zimmerman, J.A., González, M.A., de la Figuera, J.,Hamilton, J.C., Pai, W.W., and Rojo, J.M., 2002, *Phys. Rev. Lett*., **88**, 36101.
[8]. Li, J., Van Vliet, K.J., Zhu, T., Yip, S., and Suresh, S., 2002, *Nature*, **418**, 307.
[9]. Knap, J., Ortiz, M., 2003, *Phys. Rev. Lett*., 90, 226102.
[10]. H. Y. Liang, C. H. Woo, Hanchen Huang, A. H. W. Ngan, T. X. Yu, (2004) unpublished work.
[11]. Egami, T., Maeda, K., and Vitek, V., 1980, *Phil. Mag. A*, **41**, 883.
[12]. Suresh, S., Nieh, T.G., and Choi, B.W., 1999, *script. mater*., **41**, 951.
[13]. Kiely, J.D., Jaraush, K.F., Houston, J.E., and Russell, P.E., 1999, *J. Mater. Res.*, **14**, 2219.